REPORT DOCUMENTATION PAGE

Form Approved
OMB No. 0704-0188

1. REPORT DATE *(DD-MM-YYYY)*	2. REPORT TYPE	3. DATES COVERED *(From - To)*
30-Sep-2009	REPRINT	

4. TITLE AND SUBTITLE
NUMERICAL MODELING OF S-WAVE GENERATION BY FRACTURE DAMAGE INUNDERGROUND NUCLEAR EXPLOSIONS

5a. CONTRACT NUMBER
FA8718-08-C-0026

5b. GRANT NUMBER

5c. PROGRAM ELEMENT NUMBER
62601F

6. AUTHOR(S)
Charles G. Sammis[1], Harsha S. Bhat[1,2], and Ares J. Rosakis[2]

5d. PROJECT NUMBER
1010

5e. TASK NUMBER
SM

5f. WORK UNIT NUMBER
A1

7. PERFORMING ORGANIZATION NAME(S) AND ADDRESS(ES)

University of Southern California (LA)
837 West Downey Way
Los Angeles, CA 90089-1147

8. PERFORMING ORGANIZATION REPORT NUMBER

9. SPONSORING / MONITORING AGENCY NAME(S) AND ADDRESS(ES)
Air Force Research Laboratory
29 Randolph Road
Hanscom AFB, MA 01731-3010

10. SPONSOR/MONITOR'S ACRONYM(S)
AFRL/RVBYE

11. SPONSOR/MONITOR'S REPORT NUMBER(S)
AFRL-RV-HA-TR-2009-1080

12. DISTRIBUTION / AVAILABILITY STATEMENT
Approved for Public Release; Distribution Unlimited.

University of Southern California[1] and California Institute of Technology[2]

13. SUPPLEMENTARY NOTES
Reprinted from: Proceedings of the 2009 Monitoring Research Review – Ground-Based Nuclear Explosion Monitoring Technologies, 21 – 23 September 2009, Tucson, AZ, Volume III pp 557 - 565.

14. ABSTRACT

The quasi-static micromechanical damage mechanics originally formulated by Ashby and Sammis (PAGEOPH, 1990) has been expanded in three important ways: 1) An energy density function has been derived that allows a self-consistent inclusion of the effects of dynamic damage evolution on the elastic and anelastic response, 2) whereas the Ashby/Sammis model was only applicable to the case where the initial cracks are all parallel and the same size, we can now include a specified distribution of initial crack sizes with random azimuthal orientation about the loading axis, and 3) we allow for yielding of the weaker minerals in granite at relatively low stress levels which produce strong nonlinearity in the failure envelope and stress-strain curve. This new damage mechanics is validated using published experimental data for Westerly granite. In collaboration with the mechanics group at U.C. Santa Barbara, we have built our new damage mechanics into the commercial finite element program ABAQUS and used it to simulate an explosion in damaged rock. We find that an explosion in a pre-stressed medium or one that contains anisotropic initial damage generates strong *S*-wave radiation in agreement with previous simpler calculations by Johnson and Sammis (PAGEOPH, 2001) and experimental observations in damaged photoelastic plates.

15. SUBJECT TERMS
Explosion damage, Explosion shear waves, Explosion effects prediction

16. SECURITY CLASSIFICATION OF:			17. LIMITATION OF ABSTRACT	18. NUMBER OF PAGES	19a. NAME OF RESPONSIBLE PERSON
a. REPORT	b. ABSTRACT	c. THIS PAGE			Robert J. Raistrick
UNCLAS	UNCLAS	UNCLAS	SAR	9	19b. TELEPHONE NUMBER *(include area code)*

NUMERICAL MODELING OF S-WAVE GENERATION BY FRACTURE DAMAGE IN UNDERGROUND NUCLEAR EXPLOSIONS

Charles G. Sammis[1], Harsha S. Bhat[1,2], and Ares J. Rosakis[2]

University of Southern California[1] and California Institute of Technology[2]

Sponsored by the Air Force Research Laboratory

Award No: FA8718-08-C-0026
Proposal No. BAA08-82

ABSTRACT

The quasi-static micromechanical damage mechanics originally formulated by Ashby and Sammis (PAGEOPH, 1990) has been expanded in three important ways: 1) An energy density function has been derived that allows a self-consistent inclusion of the effects of dynamic damage evolution on the elastic and anelastic response, 2) whereas the Ashby/Sammis model was only applicable to the case where the initial cracks are all parallel and the same size, we can now include a specified distribution of initial crack sizes with random azimuthal orientation about the loading axis, and 3) we allow for yielding of the weaker minerals in granite at relatively low stress levels which produce strong nonlinearity in the failure envelope and stress-strain curve. This new damage mechanics is validated using published experimental data for Westerly granite. In collaboration with the mechanics group at U.C. Santa Barbara, we have built our new damage mechanics into the commercial finite element program ABAQUS and used it to simulate an explosion in damaged rock. We find that an explosion in a pre-stressed medium or one that contains anisotropic initial damage generates strong *S*-wave radiation in agreement with previous simpler calculations by Johnson and Sammis (PAGEOPH, 2001) and experimental observations in damaged photoelastic plates.

OBJECTIVES

The overall objective of this research program has been to understand and quantify the extent of fracture damage in the non-linear source region of an underground nuclear explosion and to assess its effect on the radiation of seismic energy to the far field. Of particular interest is the generation of high-frequency shear waves that may affect regional discrimination and yield estimation. The specific objective of this year's research has been to build on the work of Deshpande and Evans (2008), to extend the micromechanical damage mechanics originally formulated by Ashby and Sammis (1990), and to incorporate it in numerical models that simulate underground explosions.

RESEARCH ACCOMPLISHED

Our major accomplishment this year has been to make three important improvements in the micromechanical damage mechanics developed by Ashby and Sammis (1990) and expanded by Deshpande and Evans (2008). First, we dropped the assumption, implicit in both formulations, that the growing wing cracks are all parallel and all the same size, which strongly affects the interaction between the growing wing cracks that leads to failure. Second, we calculated the change in elastic energy density associated with the growing wing cracks in a less approximate way than that used by Deshpande and Evans (2008), which has led to a more accurate stress-strain simulation. Third, we account for the fact that granite is multimineralic and that yielding in the weaker minerals begins at relatively low stress levels.

We have built this new mechanics into the dynamic finite element code ABAQUS and produced some initial simulations of damage evolution during an underground explosion. Finally, we have begun experiments in which a hyper-velocity impact is used to simulate an explosion. A hyper-velocity impact creates a much higher energy density at the source than does an exploding wire, which allows us to better scale the damage process from the field to the lab.

Improvments to the Ashby Sammis (1900) Micromechanical Damage Mechanics

Ashby and Sammis (1990) (hereafter referred to as A&S) formulated a micromechanical damage mechanics based on the nucleation, growth and interaction of tensile "wing cracks" nucleated at the tips of an initial distribution of penny-shaped microcracks. The basic elements of their model are illustrated in Figure 1.

A&S demonstrated that their model gives an adequate description of the failure envelope (σ_1 vs σ_3 at failure) at low confining pressures, σ_3, for a wide range of rocks loaded in triaxial compression ($\sigma_1 < \sigma_2 = \sigma_3$, where compression is taken as negative).

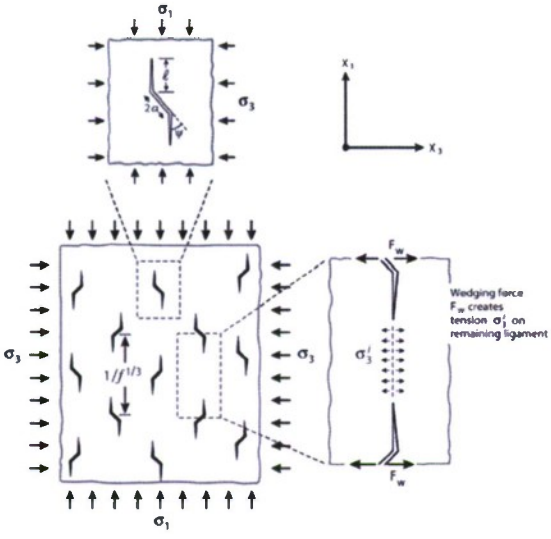

Figure 1. Geometry of damage mechanics model (from Deshpande and Evans, 2008). And initial distribution of flaws of radius *a* are loaded in compression. Sliding on the initial flaws nucleates tensile "wing cracks" at their tips of length *l*. The wedging force produced by the angle cracks creates tension on the remaining ligament creating a positive feedback that leads to instability and failure. The initial damage is defined as $D_o = \frac{4}{3}\pi(\alpha a)^3 N_V$ **where** N_V **is the volume density of initial flaws. Damage increases as the wing cracks grow according to** $D = \frac{4}{3}\pi(l+\alpha a)^3 N_V$.

However, the failure envelope predicted by this model is nearly linear while the observed failure envelope for Westerly granite is very non-linear, especially at high confining pressures (see Figures 2 and 3). A&S hypothesized that this nonlinearity is caused by a transition to plastic deformation at very high confining pressures. We shall show in a subsequent section that the broad transition zone in Fig. 3 is due to the multimineralic composition of Westerly granite where the weaker minerals yield at relatively low stress levels.

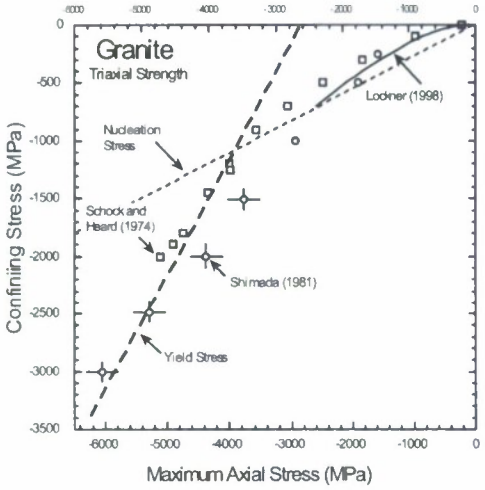

Figure 2. Failure envelope for Westerly granite under triaxial loading $\sigma_1 < \sigma_2 = \sigma_3$. Sources of data are labeled. The heavy dashed line shows the yield stress for quartz. The light dashed line shows the stress state at which the initial flaws nucleate wing cracks. Note that no additional damage can occur for confining stress greater than about 1000 MPa (confining pressure is taken as negative).

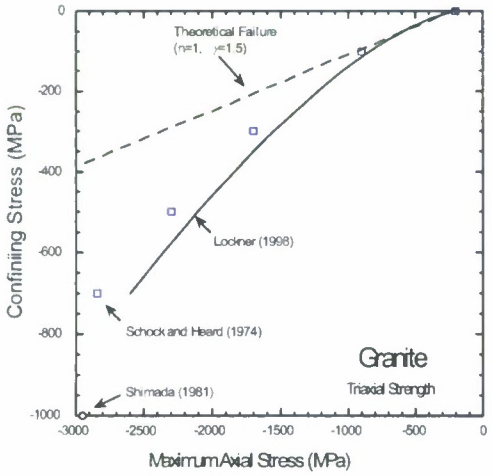

Figure 3. Enlarged view of failure envelope in Fig. 2 near $\sigma_3 = 0$. The dashed curve is the theoretical failure envelope when all flaws are the same size. The variable γ is a correction for a distribution or crack orientations defined in the text. Note that the departure from linearity begins at $\sigma_3 \approx 100$ MPa. The key question is whether this deviation from linearity is due to a distribution of sizes of starter flaws or the mineralic heterogeneity of Westerly granite where the weaker grains begin to yield at significantly

Johnson and Sammis (2001) used the A&S damage mechanics to model the 1 kt chemical explosion detonated in September 1993 as part of the Non-Proliferation Experiment (NPE). They found that the explosion induced fracture damage to a distance up to ten times the cavity radius. More importantly, they found that the damage itself generated significant "secondary radiation" of *P* and *S* waves in the seismic band. However, the A&S formulation they used is incomplete. Although it allows an estimate of the evolving damage and predicts failure, it does not provide an estimate of the stress-strain behavior associated with the increasing damage. For their numerical simulations, Johnson and Sammis (2001) used an empirical stress-strain relation borrowed from soil mechanics, which was not connected to the damage model.

Deshpande and Evans (2006) (hereafter referred to as D&E) extended the A&S damage mechanics to include stress-strain behavior by deriving the internal energy density as a function of stress, which they then differentiated to find the strain. They wrote the energy density W as

$$W = W_o + N_V \Delta W_1 + N_V \Delta W_2 \qquad (1)$$

where W_o is the elastic energy density, ΔW_1 is the change in energy density per crack due to sliding on the preexisting cracks, and ΔW_2 is the change in energy density per crack due to the growth of wing cracks. The axial strain for any stress state (σ_1, σ_3) may be calculated from the energy density as

$$\varepsilon_1 = \frac{\partial W(\sigma_1, \sigma_3)}{\partial \sigma_1} \tag{2}$$

The first two terms in the energy density are quadratic in σ_1 and thus give a linear stress-strain curve on differentiation. The second term reduces the effective Young's modulus, as in O'Connell and Budiansky (1974). The third term is not quadratic and produces curvature in the stress-strain curve, in the sense of the observations in Figures 2 and 3. The question is, how much curvature?

The perturbation in internal energy due to the growth of wing cracks can be written

$$\Delta W_2 = \frac{2\pi}{E_o} \int_{\alpha a}^{l+\alpha a} K_I^2 r dr \tag{3}$$

where K_I is the mode I stress intensity factor at the tips of the wing cracks and l, α, and a are defined in Figure 1. A&S derive an analytical expression for K_I that can be integrated to find ΔW_2.

In their formulation, D&E simplify the integration in eqn. (3) by assuming the wing cracks grow at a fixed value of l/a and write

$$\Delta W_2 = \frac{2\pi}{E_o} \int_0^a K_I^2 r dr \tag{4}$$

Since K_I^2 is a constant for fixed l/a, they can remove it from the integral giving a very simple result. However, we have shown (Sammis et al., 2009) that this simplification is too extreme in that ΔW_2 becomes independent of the evolving damage. Hence in the D&E approximation, wing-crack growth produces zero additional strain when the strain is calculated as $\varepsilon_1 = \partial W / \partial \sigma_1$ according to equation (2).

However, Sammis et al. (2009) point out that $K_I = K_{Ic}$ (its critical value) during quasi-static crack growth so it can be removed from the integral in eqn. (3) giving an equally simple result

$$\Delta W_2 = \frac{3}{4} \frac{K_{Ic}^2 D_o}{E_o \alpha a} \left[\left(\frac{D}{D_o} \right)^{2/3} - 1 \right], \tag{5}$$

where $D_o = \frac{4}{3}\pi(\alpha a)^3 N_V$ is the initial damage associated with the angled cracks, $D_o = \frac{4}{3}\pi(l + \alpha a)^3 N_V$ is the current damage, and N_V is the volume density of initial flaws. Since D increase with σ_1 up to failure, the nonlinear strain contributed by the growing wing cracks is non-zero.

Even with this correction, we found that the damage model fails to predict the observed curvature in the failure envelope. Figure 3 compares the theoretical and observed failure envelopes which diverge at confining pressures above about 100 MPa. Figure 4 shows the nonlinear portion of the stress strain curve for Westerly granite at a confining pressure of 200 MPa from Lockner (1998). The extra strain associated with the growth of wing cracks (the only nonlinear contribution in the model) is more than an order of magnitude smaller than the measured nonlinearity.

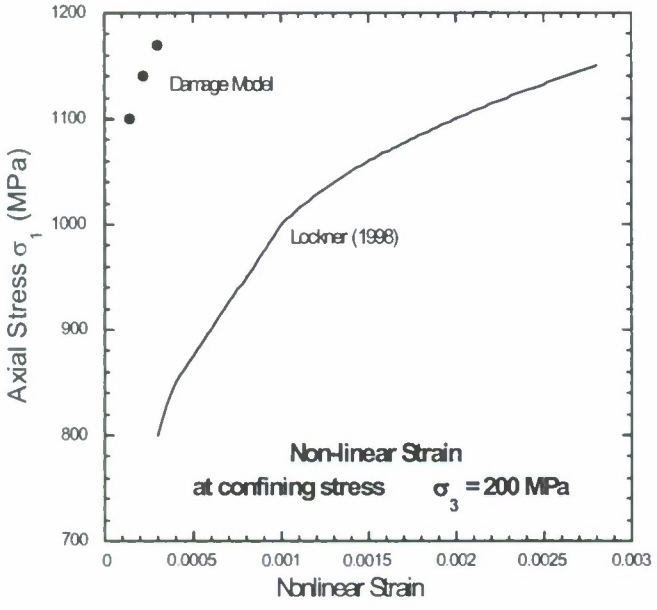

Figure 4. Non-linear strain in Westerly granite at a confining pressure of 200 MPa (redrawn from Lockner, 1998). Note that significant non-linear strain begins at an axial stress equal to about half of the failure stress and that the non-linear portion of the strain at failure is about 0.003. The non-linear strain associated with the growth of wing cracks (solid circles) is about one order of magnitude smaller.

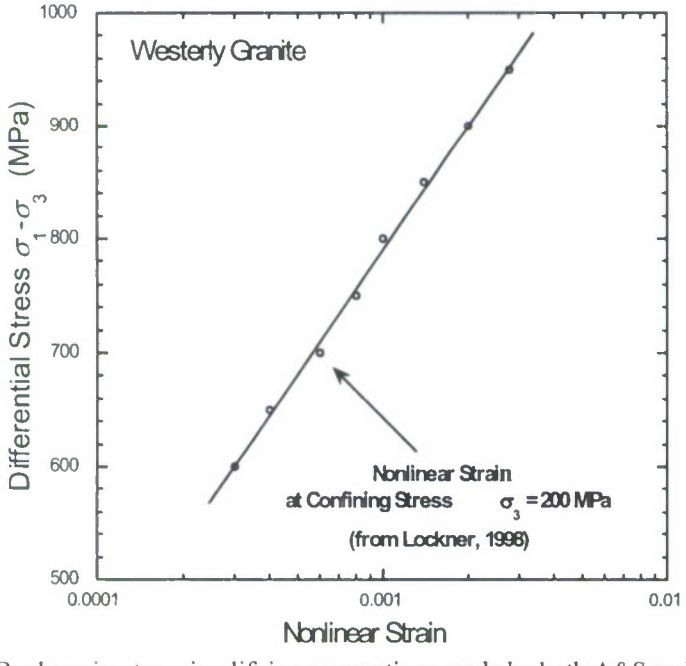

Figure 5. Same as Fig.4 but with logarithmic nonlinear strain and differential stress. The straight line implies that the stress-strain curve is of the form

$$\sigma_1 - \sigma_3 = A \log \varepsilon_{nonlinear} + B$$

By dropping two simplifying assumptions made by both A&S and D&E the damage meehanies can produee more nonlinearity in the failure envelope: 1) we no longer assume that all the initial flaws are parallel and 2) we no longer assume that all flaws are the same size. We can drop the assumption that all flaws are parallel by modifying the interaetion term. We still assume that all flaws are all at an angle α to the x_1 loading axis but allow the x_2 and x_3 components of their normal veetors to be randomly distributed. The effect is to reduee both the wedging force and average eross-seetion area supporting the interaetion. We drop the seeond assumption that all flaws are the same size by simply keeping track of the growth and interaction of a distribution of initial flaw sizes. We ehose the distribution measured in Westerly granite by Hadley (1976) shown in Figure 6. This is a bimodal distribution having a population of flaws at the grain boundary seale (about 1 mm) and a seeond power-law (fraetal) distribution of microcracks at the 10–100 micron scale.

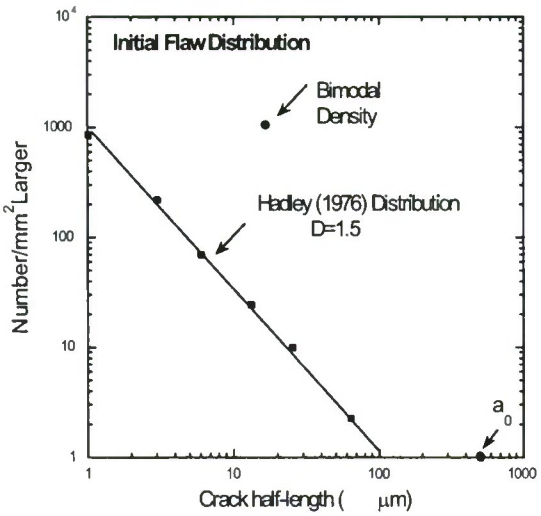

Figure 6. Initial flaw distribution in Westerly granite measured by Hadley (1976). This is a bimodal distribution with flaws of radius a near the size of the grain boundaries (about 0.5 mm) and a second fractal population of microcracks with radii less than 100 microns. The point labeled "Bimodal Density" is the density of smaller flaws required to produce the observed curvature in the failure envelope. However, even with this larger density, the stress-strain curve does not have enough nonlinearity.

Although both corrections produced more damage prior to failure, the total strain at failure (as shown by the closed circles in Fig. 4) was still only about $5x10^{-4}$, a full order of magnitude smaller than the measured value. These corrections also failed to produce the observed curvature in the failure envelope in Figures 2 and 3. Even with the extra damage, the failure envelope was nearly linear. We could simulate the observed curvature in the failure envelope by increasing the density of microfractures relative to the grain boundaries (closed circle labeled "bimodal density" in Fig. 6), but this required micro-fracture densities two orders of magnitude larger than those measured by Hadley (1976).

One way that we can generate the observed nonlinearity in both the failure envelope and stress-strain curves is to account for the multimineralic composition of Westerly granite. If the yield stress in the Feldspars and micas is significantly less than the yield stress of quartz, then nonlinear flow of the weak minerals will transfer stress to the quartz, which will carry a stress well above the average macroscopic loading stress. The quartz grains fail at the higher stress levels predicted by brittle damage mechanics, but the apparent macroscopic failure stress, being an average of the flow-stress of the weaker minerals and the brittle strength of quartz, is much smaller, as observed.

A simple model that can produce the required curvature in both the failure envelope and stress-strain curve is shown in Figure 7. Although we have not yet fully explored this model the preliminary results are encouraging. As illustrated in Figure 8, the observed failure stress lies between the flow stress of the weaker minerals and the elastic failure of quartz. Moreover, the extra elastic strain in the stronger mineral as it is loaded by the flow of the weaker ones is close to the observed nonlinear stain at failure in Figure 4.

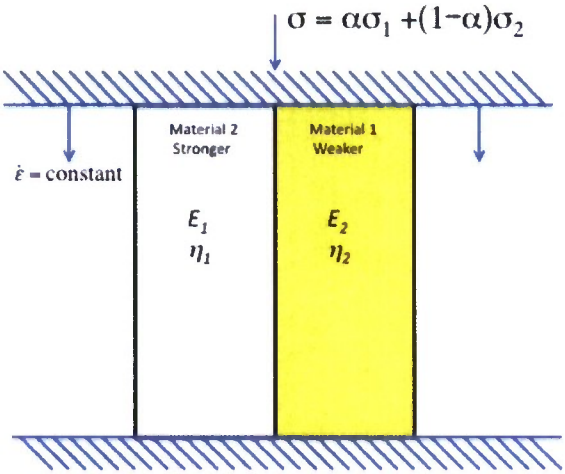

Figure 7. Simple model of a two-mineral rock loaded in compression at a constant loading rate $\dot{\varepsilon} = \text{constant}$. The loading stress σ is the average of the stresses carried by each mineral weighted according to its cross-sectional area. For the stronger mineral 1,

$$\varepsilon = \varepsilon_{1elastic} + \varepsilon_{1plastic}$$

$$\varepsilon_{1elastic} = \sigma_1 / E_1$$

$$\dot{\varepsilon}_{1plastic} = \sigma_1 / \eta_1$$

with the same expressions for the elastic and plastic strains in the weaker mineral 2.

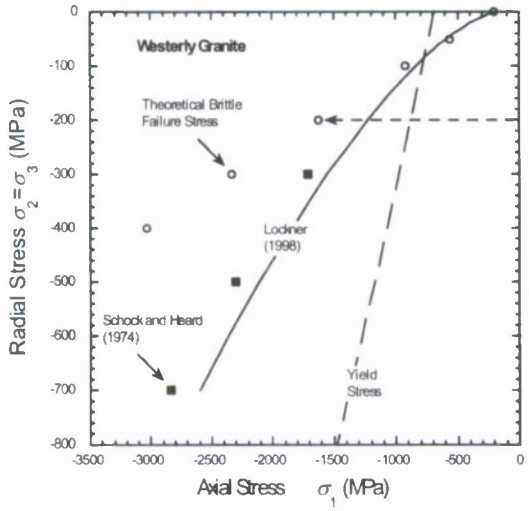

Figure 8. Failure envelope for Westerly granite. The open circles are the strength predicted by the brittle damage mechanics. Note that brittle failure is an adequate description to a confining stress of about -100 MPa. The solid curve is the failure envelope measured by Lockner (1998). The dashed arrow shows a confining stress of -200 MPa. Note that the measued failure stress is an average of the brittle failure stress predicted by damage mechanics and the flow stress of the weaker minerals.

The incorporation of damage mechanics into the ABAQUS dynamic finite element code: the numerical simulation of an underground explosion and the generation of *S* waves from the damage

Numerical calculation of this problem was done using a commercial Finite Element Package, ABAQUS. A user-defined subroutine, VUMAT, was written that incorporates the micro-mechanics based damage constitutive law described above. The model dimensions are scaled by the radius of the explosion hole, *a*. The size of the domain of computation is *120a* x *120a* (see Figure 9). This domain was finely meshed with about 120000 triangular elements. The boundary conditions applied were a constant uniaxial or biaxial loading. The initial condition for the problem was a sudden release of pressure along the inner periphery of the hole simulating an explosion. The entire calculation was done under the assumption of plane-stress conditions.

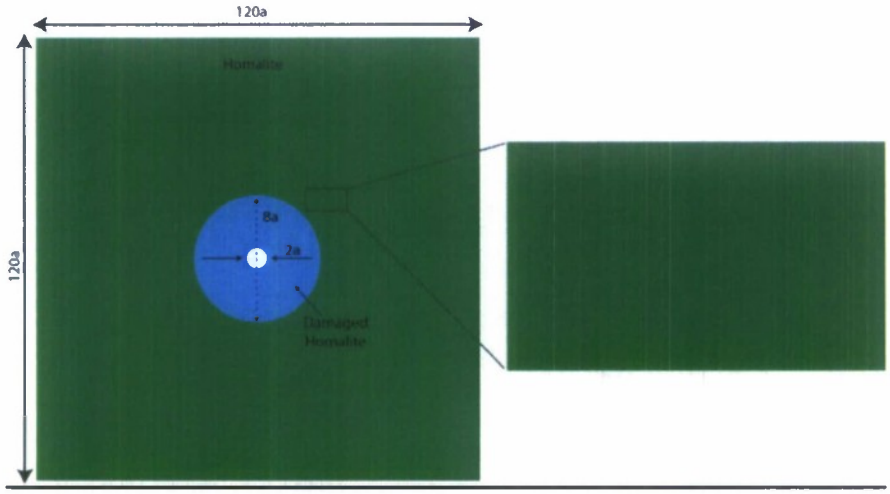

Figure 9. Geometry and mesh design for the 2D ABAQUS simulation of and explosion shown in Figure 10.

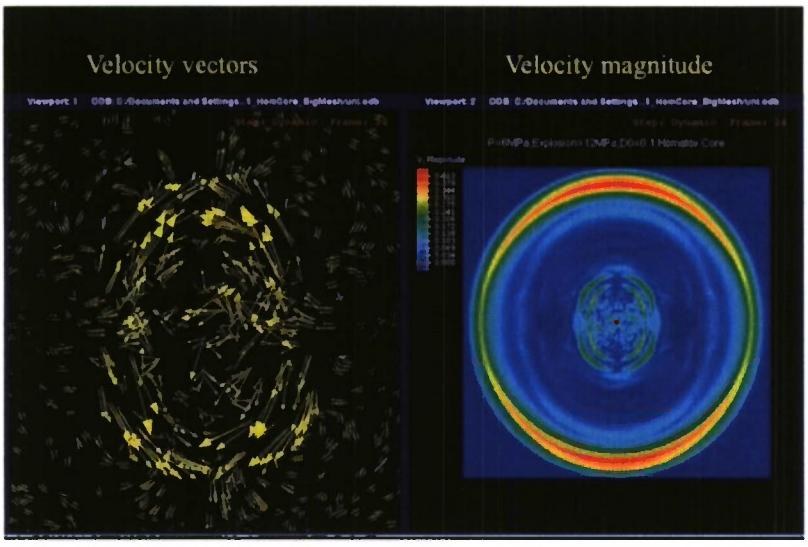

Figure 10. Velocity vectors and magnitude showing the development of S waves in the damaged area, which then propagate to the far field. These calculations used the previous D&E formulation where all initial flaws are the same size and are parallel.

The experimental simulation of an undergroud explosion using hypervelocity impact

Our experiments reported last year used a wire that was exploded by a high-voltage pulse. When this explosion occurred in the center of a damaged region under non-hydrostatic load, strong *S* waves were observed to emerge. However, the explosion was not sufficiently strong to nucleate new damage from the existing cracks. One was to produce a more intense source (in 2D experiments) is by using a high-velocity impactor.

Figure 11 shows the pattern of radial and circumferential fractures generated in a Homalite plate by a high-velocity impactor. Note the similarity to fracture patterns produced by underground explosions. We are currently developing the experimental capability to perform this experiment on loaded plates and to measure the resultant *S*-wave radiation.

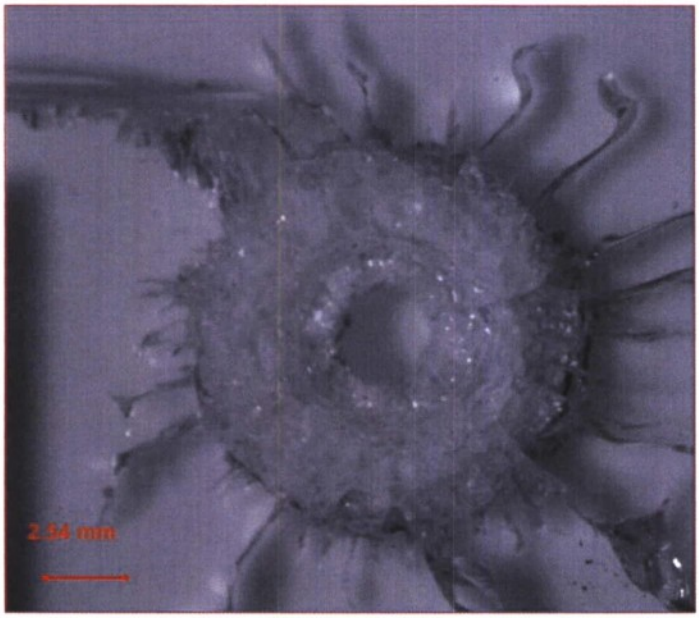

Figure 11. Fracture pattern generated by a high-velocity impact on an undamaged Homalite plate. Note that the pattern of radial and circumferential fractures is the same as that observed in underground explosions. The impactor was an equidimensional nylon slug, (L/D ~ 1, D=0.070") with an impact velocity of 6.48 km/s

CONCLUSIONS AND RECOMMENDATIONS

Our primary achievement this year has been the following significant improvements in the Ashby and Sammis (1990) damage mechanics:

1) We have derived an expression for changes in the internal energy density associated with the growth of damage. Although we followed the method developed by Deshpande and Evans (2008), we corrected fundamental errors in their formulation.

2) We extended the previous formulations to allow non-parallel initial fractures.

3) We extended the previous formulations to allow a range of initial flaw sizes.

Even with these improvements, we were unable to reproduce the observed failure envelope and stress strain curves for Westerly granite for confining pressures above about 100 MPa. We conclude that a simulation of the deformation of granite at high confining stress requires that we allow for plastic flow of the weaker constituent minerals.

We have built our damage mechanics into the ABAQUS finite element code and simulated a 2D explosion in damaged Homalite that generated significant *S* wave energy in the damage material. We are currently including the above improvements in the code, after which we will continue with the simulations of explosions.

Finally, we have begun 2-D experiments that use a high-velocity impact to simulate an explosion. The higher energy density in the impact does far more damage than does the exploding wire used in our prior experiments, which should allow us to better explore the seismic radiation generated by the growth of new damage.

ACKNOWLEDGEMENTS

We wish to thank Vikram Deshpande for his assistance in building our damage mechanics into the ABAQUS numerical code.

REFERENCES

Ashby, M. F. and C. G. Sammis (1990). The damage mechanics of brittle solids in compression, *PAGEOPH* 133: 489–521.

Brace, W. F. (1965). Some new measurements on linear compressibility of rocks, *J. Geophys. Res.* 70: 391–398.

Deshpande, V. S. and A. G. Evans (2008). Inelastic deformation and energy dissipation in ceramics: A mechanism-based constitutive model, *J. Mechanics and Physics of Solids* 56: 3077–3100.

Hadley, K. (1976). Comparison of calculated and observed crack densities and seismic velocities in Westerly granite *J. Geophys. Res* 81: 3484–3494.

Johnson, L. R. and C. G. Sammis (2001). Effects of rock damage on seismic waves generated by explosions, *PAGEOPH*, 158, 1869-1908.

Lockner, D.A. (1998). A generalized law for brittle deformation of Westerly granite, *J. Geophys. Res.* 103: 5107-5123.

O'Connell, R. J. and B. Budiansky (1974). Seismic velocities in dry and saturated cracked solids, *J. Geophys. Res.* 79: 5412–5426.

Sammis, C. G., H. S. Bhat, and A .J. Rosakis (2009). The micromechanics of brittle solids in triaxial compression, *J. Geophysical Res.*, submitted.